17th International Conference on Environmental Science and Technology

Athens, Greece, 1 to 4 September 2021

CO_2 Utilization for Preparation of Carbon Nanostructures

GIANNAKOPOULOU T.*, PLAKANTONAKI N., VAGENAS M., PAPAILIAS I., BOUKOS N., TODOROVA N. and TRAPALIS C.

Institute of Nanoscience and Nanotechnology, NCSR "Demokritos", Patriarhou Grigoriou & Neapoleos, 15341 Attiki, Greece

*corresponding author:
e-mail: t.giannakopoulou@inn.demikritos.gr

Abstract The CO_2 conversion to valuable materials is a challenging way to manage pollution problems. In the present work, CO_2 was used as a feedstock to synthesize solid carbon nanostructures by employing a simple magnesiothermic reduction reaction under constant gas flow in a tube furnace. It was shown that the CO_2 reduction at 675 ºC led to the simultaneous formation of different nanocarbon morphologies including graphene, tubular and spherical carbon nanostructures. The synthesized material was characterized using XRD analysis, Raman spectroscopy, SEM and TEM microscopies which demonstrated its good crystallinity and morphological diversity. Electrochemical tests were performed to evaluate specific capacitance and cycling stability of the prepared sample. The calculated values of ~ 325 F/g at scan rate 0.1 V/s revealed that the obtained nanostructures can be used as effective functional material for supercapactior applications.

Keywords: CO_2 conversion, nanocarbons, metallothermic reduction, Mg

1. Introduction

Being one of the major greenhouse gases, carbon dioxide (CO_2) is responsible for the global warming due to its constantly increasing emissions from human activities. Many efforts have been made to reduce the CO_2 emissions as well as to capture, store or convert the CO_2 into value-added materials (Khoo 2015). The CO_2 conversion into solid nanocarbons such as graphene, carbon nanotubes (CNTs) or nanofibers (CNFs) is a promising way to address the mentioned issue. Several conversion approaches like plasma methods, electrochemical reduction using molten salts and metallothermic reduction can be referenced (Li (2021), Liu 2020). The metallothermic reduction reactions typically use reactive alkali or alkaline earth metals to reduce CO_2 to carbons (Dabrowska 2012). The earliest experiments were performed in closed-type batch reactors with solid (dry ice), supercritical or gaseous CO_2 and a few reductants (i.e., Li, K, Na, Ca, etc.). The reactions required high pressures and resulted mainly in graphene-structured carbons. Recently, the controlled synthesis of nanocarbons with specific morphologies including mesoporous graphene, CNTs and hollow carbon nanoboxes was realized under constant CO_2 flow at atmospheric pressure through changing the reaction temperature (Zhang 2013). The variation in morphology was associated with different mechanisms of the nanocarbons growth over solid, liquid or gaseous Mg. Recent studies (Xing 2015, Xing 2017, Baik 2020) used mixed reductants and showed that the addition of several metals like Zn, Cu or Ni to Mg influences the porosity, graphitization degree or nanostructure of the prepared graphenic carbons. In the present paper, we investigate the reduction of gaseous CO_2 using Mg reducing agent only and demonstrate the formation of graphene as well as tubular and spherical nanocarbons at 675 ºC that is lower than the temperatures applied in the previous studies. Furthermore, the plethora of the obtained carbon nanostructures results in a supercapacitor electrode material with a highly conductive interconnected network that contributes to its superior performance.

2. Experimental

2.1. Nanostructures preparation

In a typical experiment, 0.5 g of Mg powder (Alfa Aesar, 99.8%, 325 mesh) was placed in alumina crucible and heated in tube furnace to 675 ºC, which is a slightly higher temperature than the melting point of Mg (~ 650 ºC). Heating rate of 10 ºC/min under Ar flow at 50 mL/min was applied. After reaching the desired temperature, Ar was switched to CO_2 that was flowing at 20 mL/min for 60 min. Then, CO_2 was turned off and the sample was left to cool down to the room temperature under 50 mL/min Ar flow. After the reaction, the black product was collected and stirred in 3.0 M HCl solution at ~70 ºC for 3 h to remove the unreacted Mg and the produced impurities (MgO). Finally, the mixture was washed with deionized water several times until the supernatant exhibits pH ~ 7 and dryed in furnace at 60 ºC.

2.2 Structural and morphological characterization

The X-ray diffraction (XRD) pattern of the prepared material was taken on a Siemens D500 diffractometer with a CuKα radiation source in a Bragg-Bretano geometry. The scanning velocity was 0.03º/3s. The Raman spectra were measured using an inVia Renishaw Raman

microscope equipped with an Ar+ laser excitation source (514.5 nm). The scanning electron microscopy (SEM) images were recorded with a FEI Inspect electron microscope operated at 25 kV using a secondary detector for image formation. Transmission electron microscopy (TEM) was used to examine fine details of the sample morphology utilizing a Thermo Fisher Scientific Talos F200i field emission gun TEM instrument.

2.3 Electrochemical characterization

The electrochemical measurements were performed on a Metrohm Autolab PGSTAT302 employing glassy carbon (GC), Ag/AgCl (3 M) and Pt plate as working, reference and counter electrodes, respectively. Aqueous solution of 0.5 M Na_2SO_4 was used as an electrolyte. The cyclic voltammetry (CV) measurements were done in a potential window from -1 V to +1V at several potential scan rates. The electrochemical impedance spectroscopy (EIS) was conducted in a frequency range from 0.1 Hz to 100 kHz with a sinusoidal perturbation of 10 mV. The galvanostatic charge–discharge (CH-DCH) tests were carried out at several constant current values. The electrode material was prepared by mixing 2 mg of the washed powder, 0.2 mL of ethanol, and 20 µL of nafion followed by sonication for 30 min. Then, 20 µL of the dispersion was dropped on a GC electrode and dried for 2 h at 60 ºC in a furnace. Taking into account the dimensions of the drop and GC electrode, the mass of the electrode material was calculated to be 40 µg.

3. Results and Discussion

The XRD pattern of the washed material is given in Figure 1a. The relatively strong diffraction peak (002) observed at ~ 26° corresponds to the graphite-like phase and indicates the crystalline character of the prepared material. The Raman spectra (Figure 1b) of the sample exhibit three main bands D, G and 2D characteristic to graphenic/graphitic materials, those intensities measured at different points slightly fluctuate. Thus, the intensity ratios I_D/I_G and I_{2D}/I_G representing disorder and graphitisation degrees vary from 0.69 up to 0.79 and from 0.49 down to 0.38, correspondingly. The I_{2D}/I_G values lower than 1 are an indication for presence of multilayer graphenic nanostructures (Baik 2020) and reflect good overall crystallinity of the sample, which correlates well with the XRD analysis

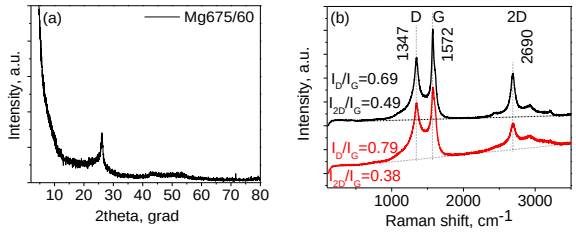

Figure 1. XRD pattern of the prepared material (a) and its Raman spectra taken at two different points for limiting (as for I_D/I_G and I_{2D}/I_G ratios) cases (b).

The SEM images given in Figure 2 evidence the formation of nanostructures with sheet-like, spherical and tubular geometry. The surface of the sheets contains a lot of pores while the spheres possess a quite smooth surface and diameter up to ~ 1.5 µm. The diameter of the tubular nanostructures is larger than 100 nm and reaches values of even 200 nm. So, it is most likely that these tubular nanostructures are not hollow and are fibers. The fibers are entangled with each other and seem to consist of distinct segments glued in chains.

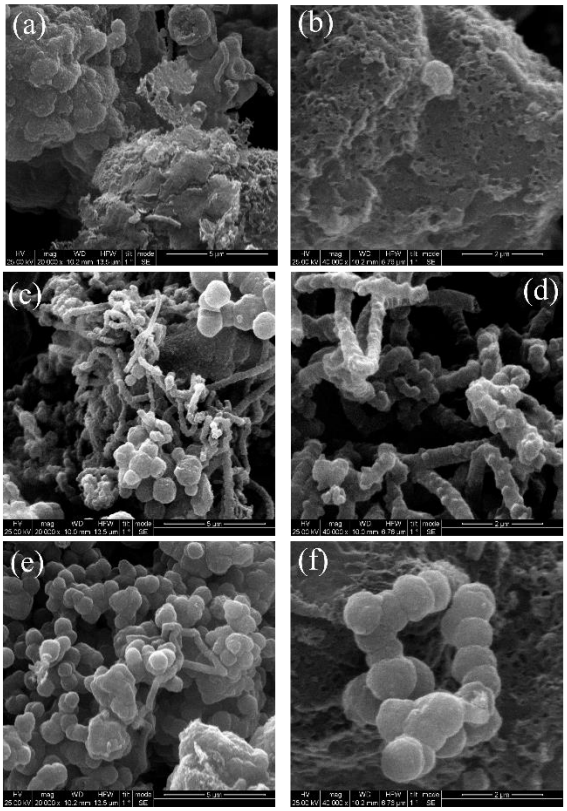

Figure 2. SEM micrographs of the prepared material: sheet-like porous agglomerates (a, b), bundles of fibers with some spheres (c, d) and a "cloud" from spheres (e, f) at different magnifications: 20000x, scale bar 5 µm (a, c, e) and 40000x, scale bar 2 µm (b, d, f).

The TEM images (Figure 3) provide more detailed information on the material morphology. Corrugated graphene sheets can be observed in Figure 3a. The presence of mesopores with dimensions of 10-20 nm in the graphene sheets is evident from the higher resolution Figure 3b. A bundle of intertwined fibrous structures and a single fiber are given in Figure 3 c and d, correspondingly. No holes are observed inside, proving that fibers but not tubes are formed in our case. The surface of the fibers is uneven and contains a lot of hooks. The image of Figure 3e demonstrates another cluster comprised of spherical and elongated nanostructures which are organized in chains or appear separately.

The electrochemical tests revealed that the electrode material possesses a typical supercapacitor behavior (Figure 4). In particular, the CV curve is nearly rectangular at lower scan rates and turns leaf-like at high

rates. The CH-DCH plot has an isosceles triangle shape and the impedance Nyquist curve is nearly parallel to the

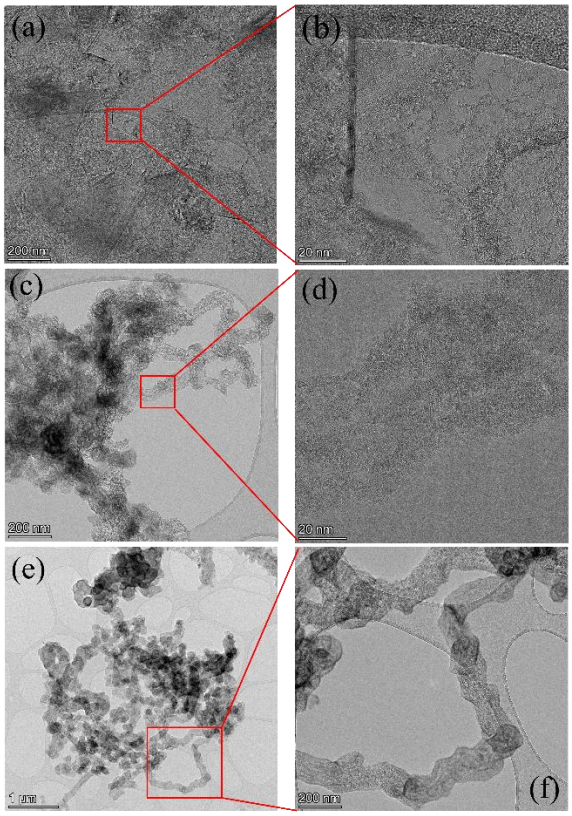

Figure 3. TEM micrographs of the prepared material: crumpled graphene sheets with mesopores (a, b), entangled fibers (c) and a fragment of fiber (d), single and jointed spherical segments (e, f) at different magnifications: 46 kx, scale bar 200 nm (a, c, f), 500 kx, scale bar 20 nm (b, d) and 11 kx, scale bar 1 μm (e).

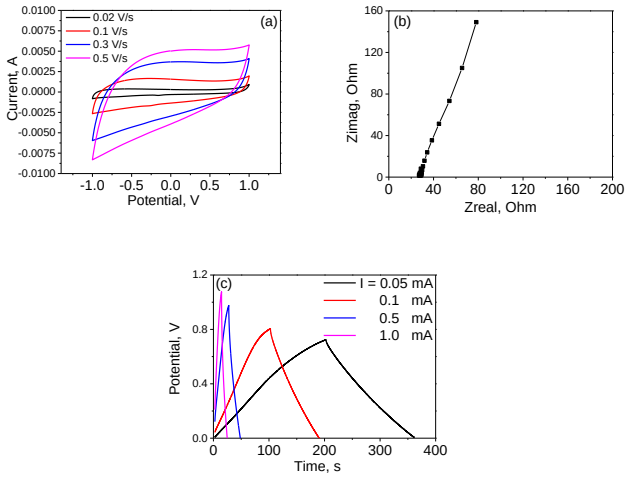

Figure 4. CV loops for different scan rates (a), CH/DCH diagram (b) and Nyquist electrochemical impedance plot (c) of the prepared electrode material measured in 0.5 M Na_2SO_4 electrolyte.

OY axis. The values of specific capacitance calculated using CV, CH/DCH and EIS are listed in Table 1. The capacitance estimated from the CV loops reaches a significant value of ~ 407 F/g at scan rate of 0.02 V/s and decrease to ~ 180 F/g at 0.5 V/s. At an intermediate rate of 0.1 V/s, the remarkable 325 F/g was recorded. The CH-DCH tests show a clear tendency of the increase in capacitance with the increase in current proving the ability of the material to accept higher currents.

Table 1. Calculated capacitance (C) of electrode material measured via different electrochemical techniques

C from CV		C from CH-DCH		C from EIS (F/g)
Scan rate (V/s)	C (F/g)	Current (mA)	C (F/g)	
0.02	407.3	0.05	290.9	
0.05	368.7	0.1	302.8	
0.1	**325.0**	0.5	334.5	266.8
0.2	267.4	1.0	336.9	
0.3	228.7			
0.5	179.9			

The capacitance value obtained through the EIS measurements is in good accordance with the results of the other techniques. The cycling stability of the material was evaluated using CV technique by applying 1000 cycles at 0.3 V/s rate. It was shown that the capacitance retention after the test was 98 %.

4. Conclusion

We have demonstrated that the metallothermic reduction of waste CO_2 using only Mg reductant at 675 °C (that is a bit higher temperature that the melting point of Mg) and slow gas rate is accompanied by the synthesis of different carbon nanostructures. The obtained material exhibits high crystallinity, low disorder and remarkable electrochemical perfomance and stability. The results prove that the chosen CO_2 reduction method is a feasible strategy to synthesize stable and high capacitance electrode materials for supercapacitor applications.

References

Baik S., Park J.H. and Lee J.W. (2020), One-pot conversion of carbon dioxide to CNT-grafted graphene bifunctional for sulfur cathode and thin interlayer of Li-S battery, *Electrochimica Acta*, **330**, 135264.

Dabrowska A., Huczko A. and Dyjak S. (2012), Fast and efficient combustion synthesis route to produce novel nanocarbons, *Physica Status Solidi B*, **249**, 2373–2377.

Khoo R.S.H, Luo. H.-K., Braunstein P. and Hor T.S.A. (2015),Transformation of CO_2 to value-added materials, *Journal of Molecular and Engineering Materials*, **3**, 1540007.

Li C., Zhang X., Wang K., Su F., Chen C.-M. and Liu F. (2021), Recent advances in carbon nanostructures prepared from carbon dioxide for high-performance supercapacitors, *Journal of Energy Chemistry*, **54**, 352–367.

Liu S, Jin Y, Bae J.-S., Chen Z., Dong P., Zhao S. and Li R. (2020), CO_2 derived nanoporous carbons for carbon capture, *Microporous and Mesoporous Materials*, **305**, 110356

Xing Z., Wang B., Gao W., Pan C., Halsted J.K., Chong E.S., Lu J., Wang X., Luo W., Chang C.-H., Wen Y., Ma S., Amine K. and Jia X. (2015), Reducing CO_2 to dense nanoporous graphene by Mg/Zn for high power electrochemical capacitors, *Nano Energy*, **1,** 600–610.

Xing Z., Gao N., Qi Y., Ji X., Liu H. (2017), Influence of enhanced carbon crystallinity of nanoporous graphite on the cathode performance of microbial fuel cells, *Carbon*, **115,** 271-278.

Zhang H., Zhang X., Sun X. and Ma Y. (2013), Shape-controlled synthesis of nanocarbons through direct conversion of CO_2, *Scientific Reports*, **3**, 3534.

Acknowledgement

The authors appreciate the financial support from the project "T1EDK-01729 CARBONGREEN" (MIS 5848538) co-financed by the European Union and Greek national funds through the Operational Program Competitiveness, Entrepreneurship and Innovation, under the call RESEARCH-CREATE-INNOVATE.